

Possible Insight to the Explosion Mechanism of Core Collapse Supernovae Through γ -ray Spectroscopy of ^{46}Cr

Chris Cousins

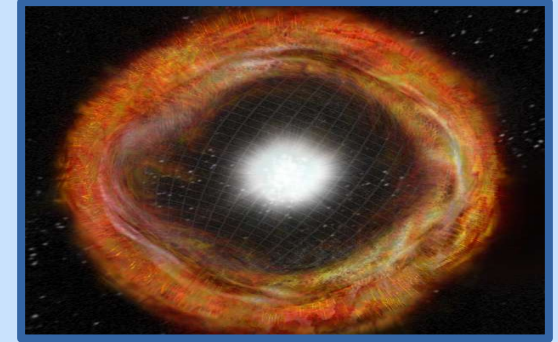
NPA-XI 2024



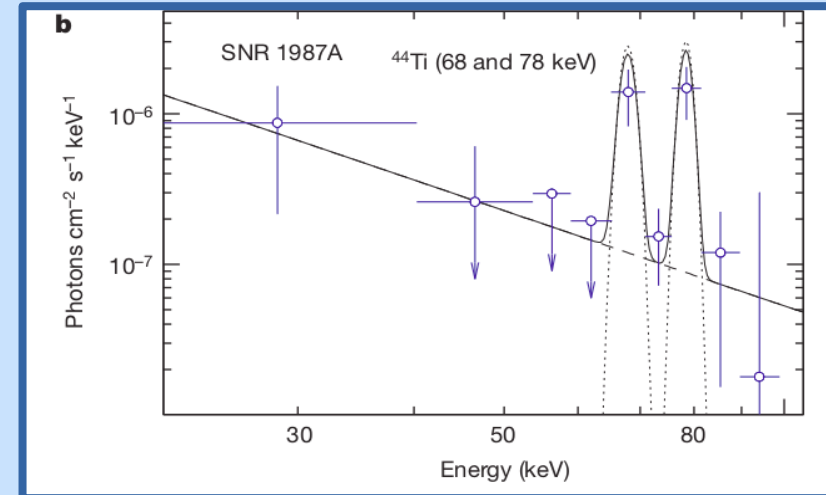
UNIVERSITY OF
SURREY

Motivation and Astrophysical Background

- Uncertainty in explosion mechanism of core collapse supernovae (CCSN)
- New insight – observing abundances of ^{44}Ti cosmic γ rays ($t_{1/2} = 60$ yr) – INTEGRAL
- Mass cut point of the star can be found – key hydrodynamic property of supernovae
- Road block! – uncertainty in nuclear reactions that destroy ^{44}Ti – most notably $^{45}\text{V}(p,\gamma)^{46}\text{Cr}$

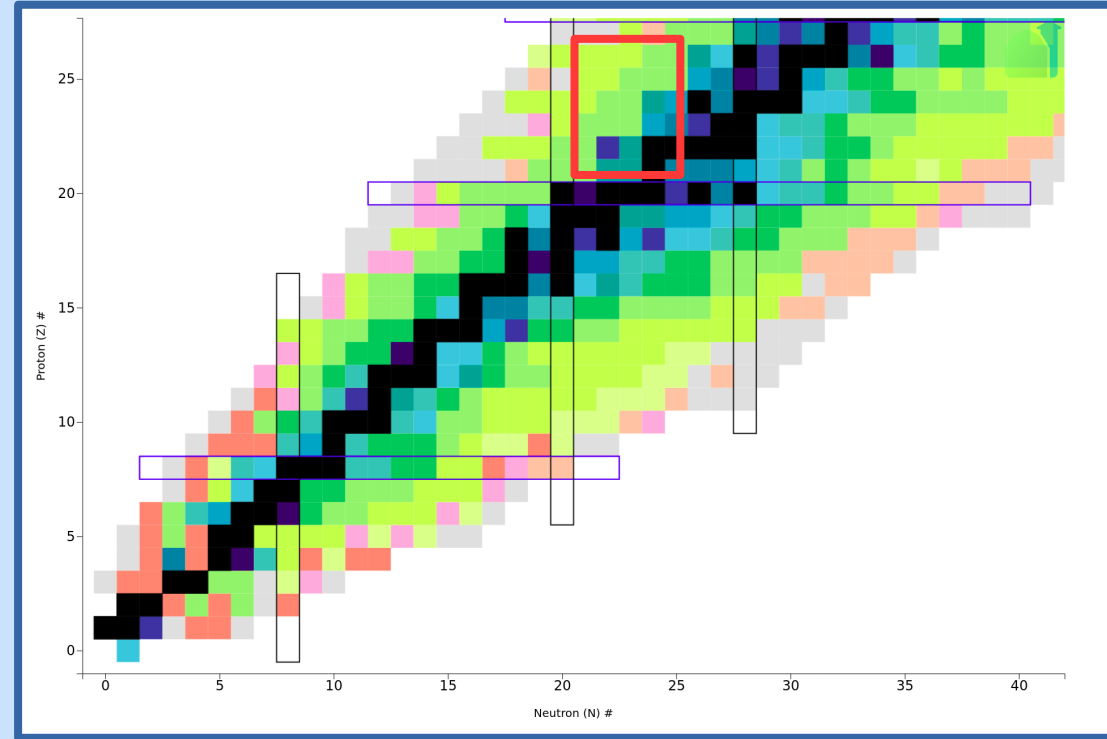


Bill Saxton (NRAO/AUI/NSF)



Importance of $^{45}\text{V}(p,\gamma)^{46}\text{Cr}$ for ^{44}Ti Destruction – α -rich Freeze Out

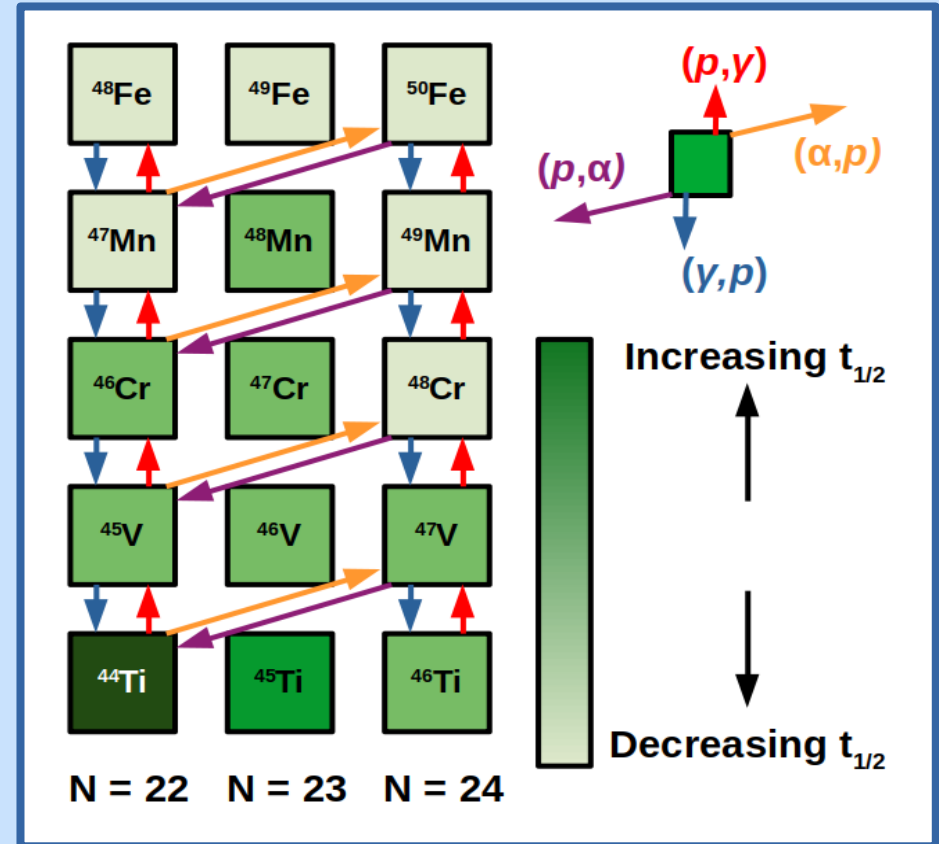
- Shock wave breaks nuclei into free nucleons and α particles
- $T \downarrow$ – Reassemble back into nuclei
- Cluster of nuclei around $f_{7/2}$ shell in equilibrium



<https://www.nndc.bnl.gov/>

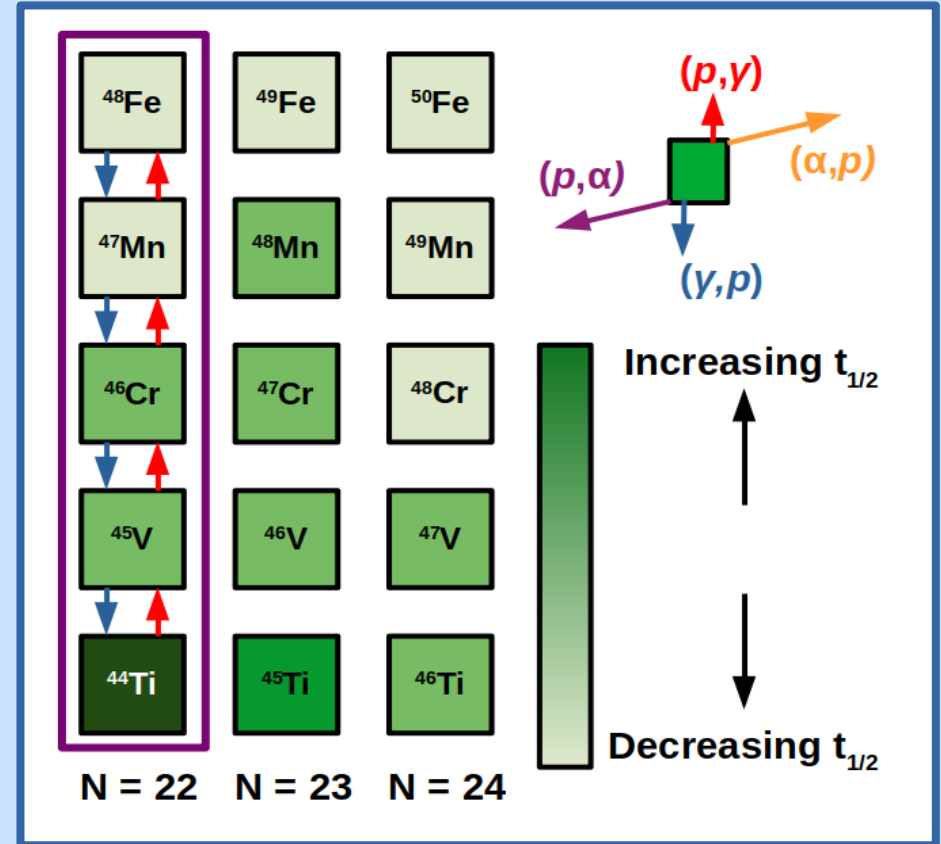
Importance of $^{45}\text{V}(p,\gamma)^{46}\text{Cr}$ for ^{44}Ti Destruction – α -rich Freeze Out

- Shock wave breaks nuclei into free nucleons and α particles
- $T \downarrow$ – Reassemble back into nuclei
- Cluster of nuclei around $f_{7/2}$ shell in equilibrium



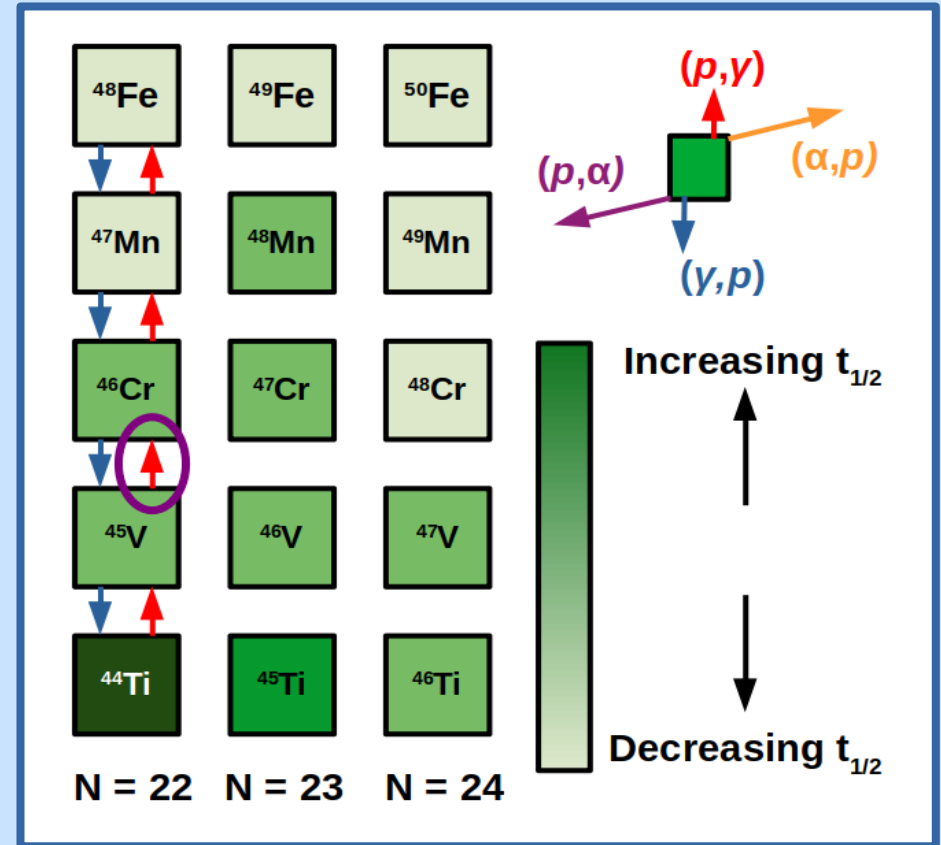
Importance of $^{45}\text{V}(p,\gamma)^{46}\text{Cr}$ for ^{44}Ti Destruction – α -rich Freeze Out

- Shock wave breaks nuclei into free nucleons and α particles
- $T \downarrow$ – Reassemble back into nuclei
- Cluster of nuclei around $f_{7/2}$ shell in equilibrium
- $T \downarrow$ – Isotone chain $N=22$ separates to form its own (p,γ) -(γ,p) equilibrium



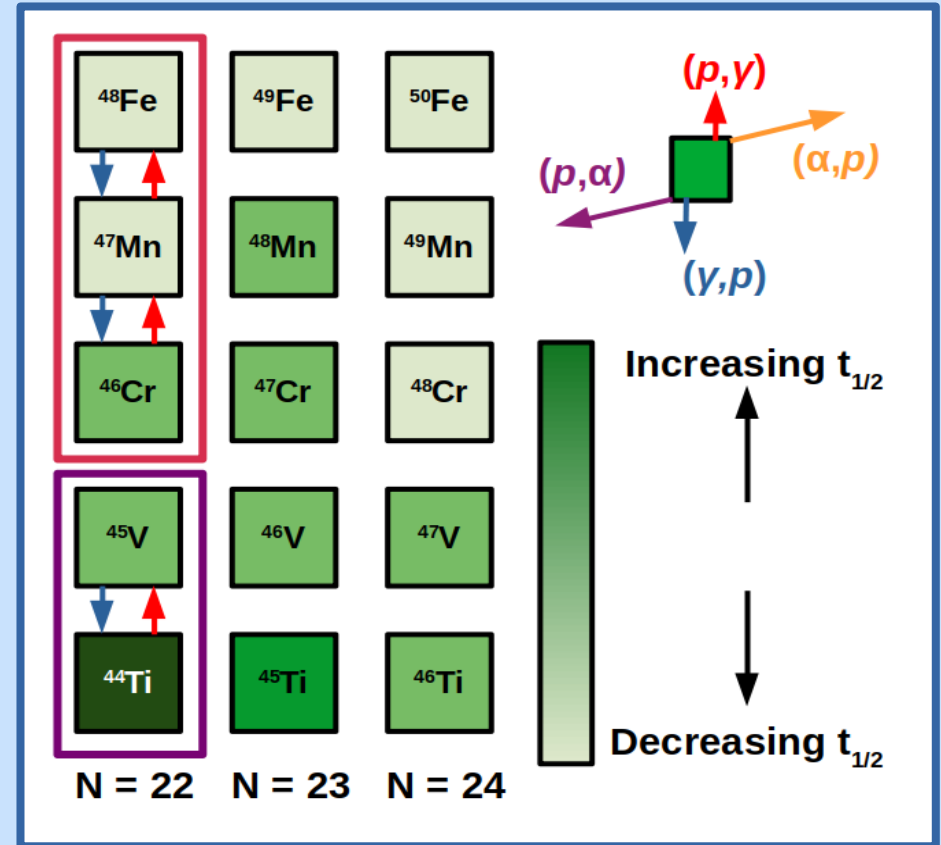
Importance of $^{45}\text{V}(p,\gamma)^{46}\text{Cr}$ for ^{44}Ti Destruction – α -rich Freeze Out

- Shock wave breaks nuclei into free nucleons and α particles
- $T \downarrow$ – Reassemble back into nuclei
- Cluster of nuclei around $f_{7/2}$ shell in equilibrium
- $T \downarrow$ – Isotone chain $N=22$ separates to form its own (p,γ) -(γ,p) equilibrium
- p -capture on ^{45}V importance identified in sensitivity studies [1] – high Q value



Importance of $^{45}\text{V}(p,\gamma)^{46}\text{Cr}$ for ^{44}Ti Destruction – α -rich Freeze Out

- Shock wave breaks nuclei into free nucleons and α particles
- $T \downarrow$ – Reassemble back into nuclei
- Cluster of nuclei around $f_{7/2}$ shell in equilibrium
- $T \downarrow$ – Isotone chain $N=22$ separates to form its own (p,γ) -(γ,p) equilibrium
- p -capture on ^{45}V importance identified in sensitivity studies [1] – high Q value
- ^{44}Ti and ^{45}V cut off from the rest of $N=22$ isotone chain – abundance determined at freeze out



Finding the Reaction Rate

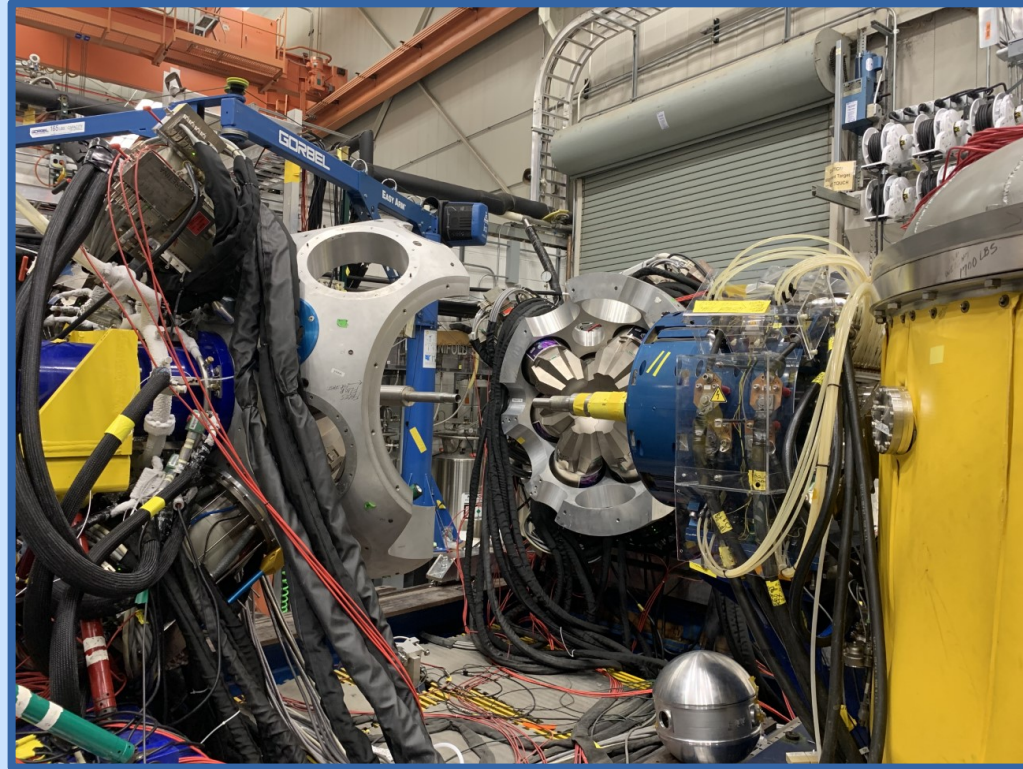
- Reaction governed by low-spin resonant states above proton separation energy ($S_p = 4882(22)$ keV)
- Performing γ -ray spectroscopy of ^{46}Cr – identifying proton-unbound resonant states
- Use resonant energies and spins to place constraints on $^{45}\text{V}(p,\gamma)^{46}\text{Cr}$ stellar reaction rate in CCSN

$$N_A \langle \sigma v \rangle = \frac{1.5399 \times 10^{11}}{(\mu T_9)^{3/2}} \sum_i (\omega\gamma)_i e^{-11.605 E_{R,i}/T_9}$$

$$(\omega\gamma)_i = \left(\frac{2J_R + 1}{(2j_0 + 1)(2j_1 + 1)} \right) \frac{\Gamma_a \Gamma_\gamma}{\Gamma_a + \Gamma_\gamma}$$

Experimental Set-Up

- GRETINA+FMA, ATLAS facility, Argonne National Lab, March 2021
 - 120 MeV ^{36}Ar beam
 - $\sim 200 \mu\text{g.cm}^{-2}$ thick ^{12}C target
 - Produces ^{46}Cr in excited states via fusion-evaporation



Fusion-Evaporation Channels

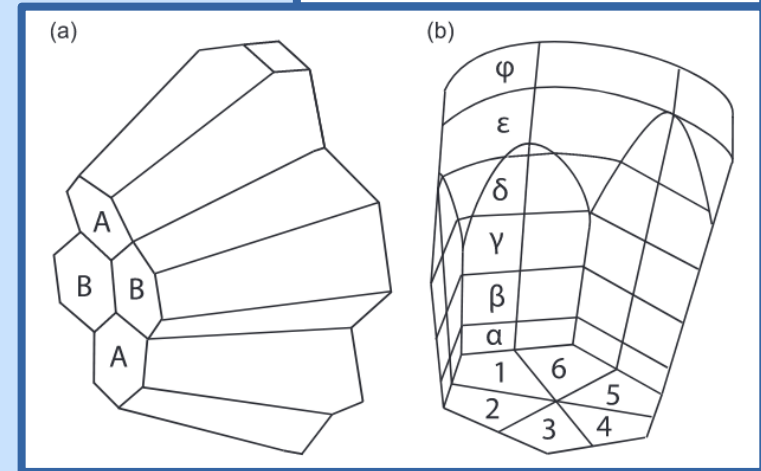
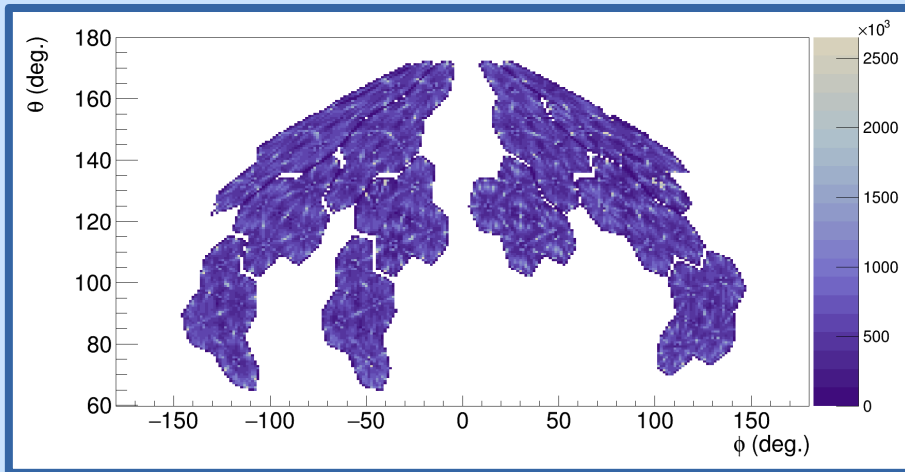
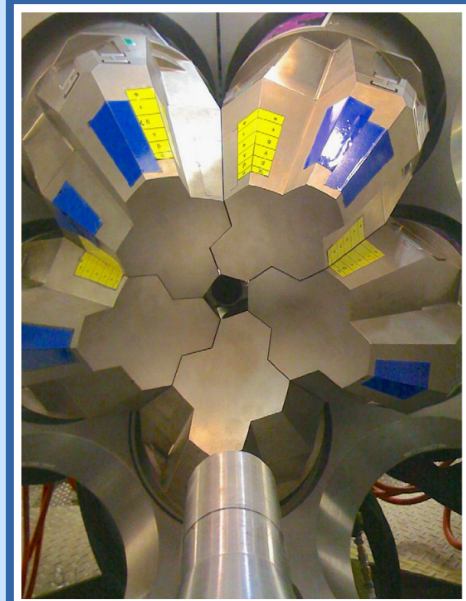
- Can't measure directly – ^{45}V $t_{1/2} \sim 500$ ms
- Fusion-evaporation reaction – $^{12}\text{C}(^{36}\text{Ar}, 2n)^{46}\text{Cr}$
- Other channels dominate this reaction – p -rich side of stability
- Contamination from oxygen on target – significant production of ^{49}Cr

Channel	Mode	Yield (%)
^{46}Ti	$2p$	28.6
^{46}V	pn	18.5
^{45}Ti	$2pn$	16.9
^{43}Sc	αp	16.4
^{40}Ca	2α	9.02
\vdots	\vdots	\vdots
^{46}Cr	$2n$	0.025

Calculations provided by PACE4

GRETINA

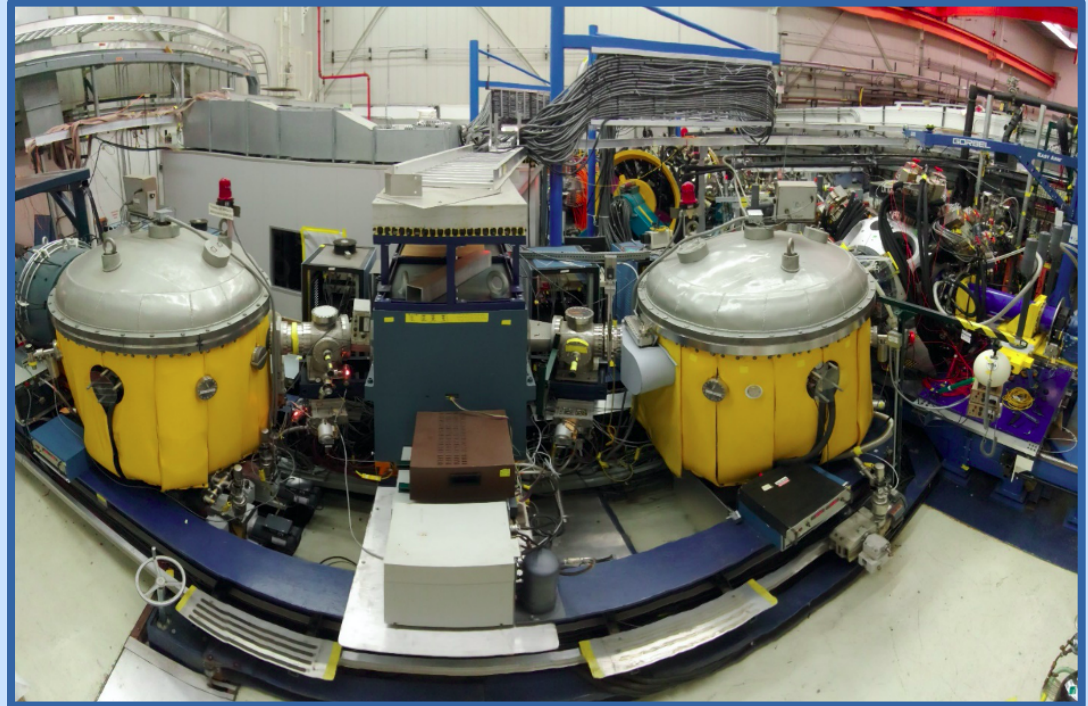
- State-of-the-art HPGe γ ray detector array
- Detect prompt γ rays in coincidence with recoils
- γ -ray tracking – reconstructs Compton scattered γ -rays – high efficiency
- Operated with 11 modules, total of 44 crystals



S. Paschalis et al. Nuclear Instruments and Methods in Physics Research Section A 709 (2013), p.44-55.

FMA

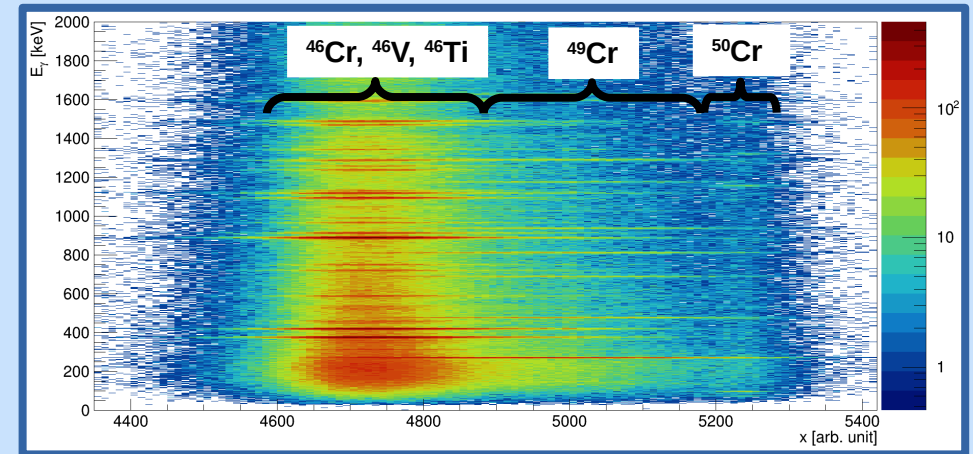
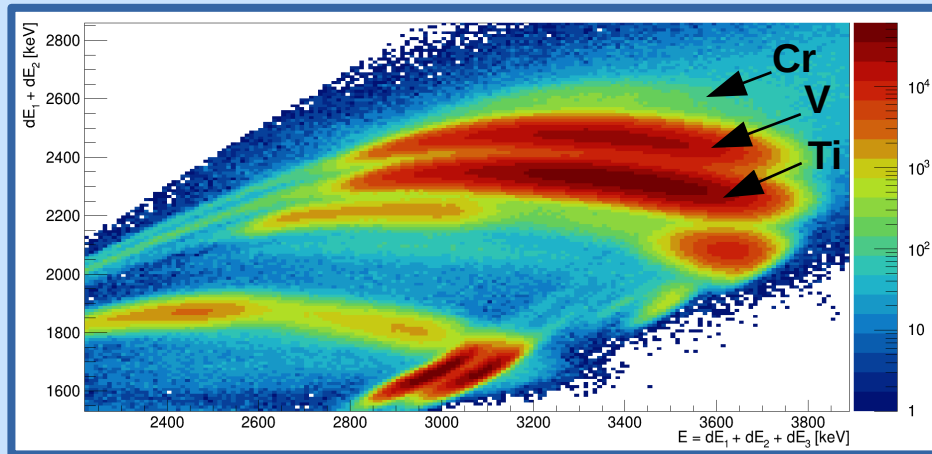
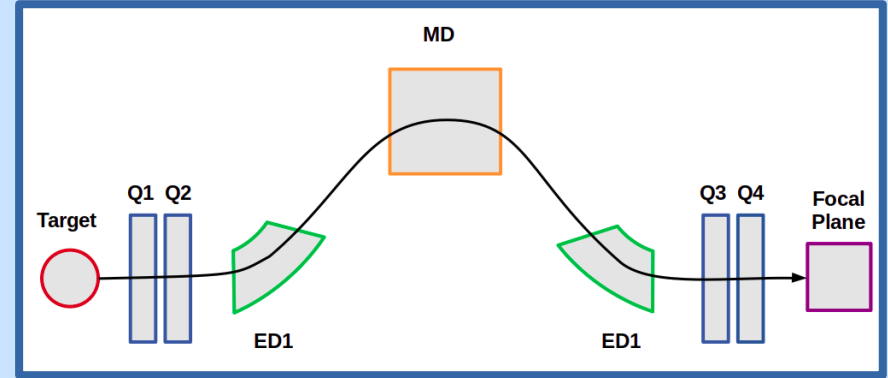
- Separates recoils by mass/charge (A/Q) at the focal plane
- Ionisation chamber – identify recoil isotopes by their Z



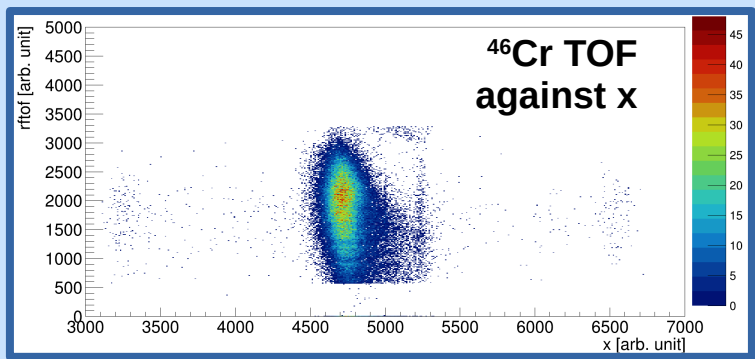
<https://www.anl.gov/phy/fragment-mass-analyzer>

Z and A/Q Gate

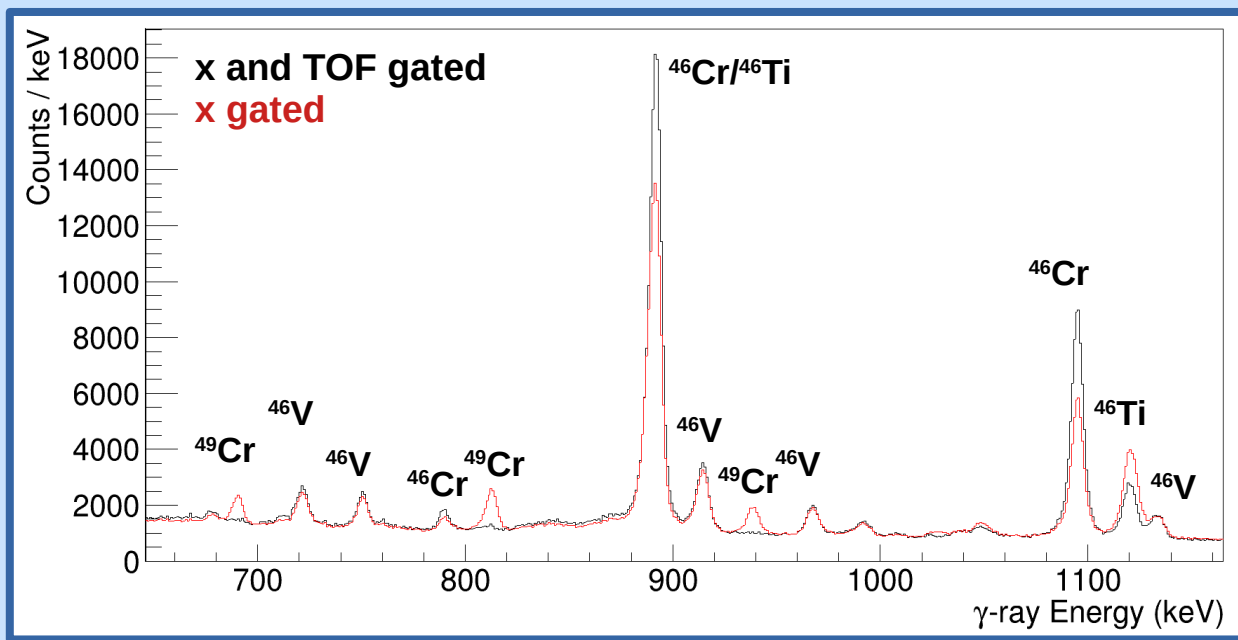
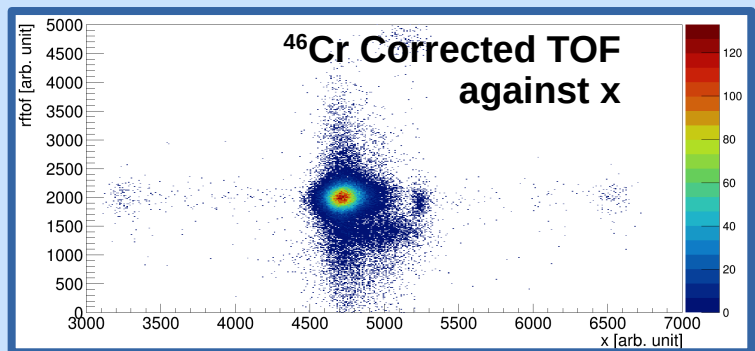
$$-\left\langle \frac{dE}{dx} \right\rangle \approx \frac{4\pi e^4}{m_e} \frac{Z_p^2}{\nu^2} \left(N_A \rho \frac{Z_t}{M_t} \right) \ln \left(\frac{2m_e \nu^2}{I} \right)$$



TOF Gate



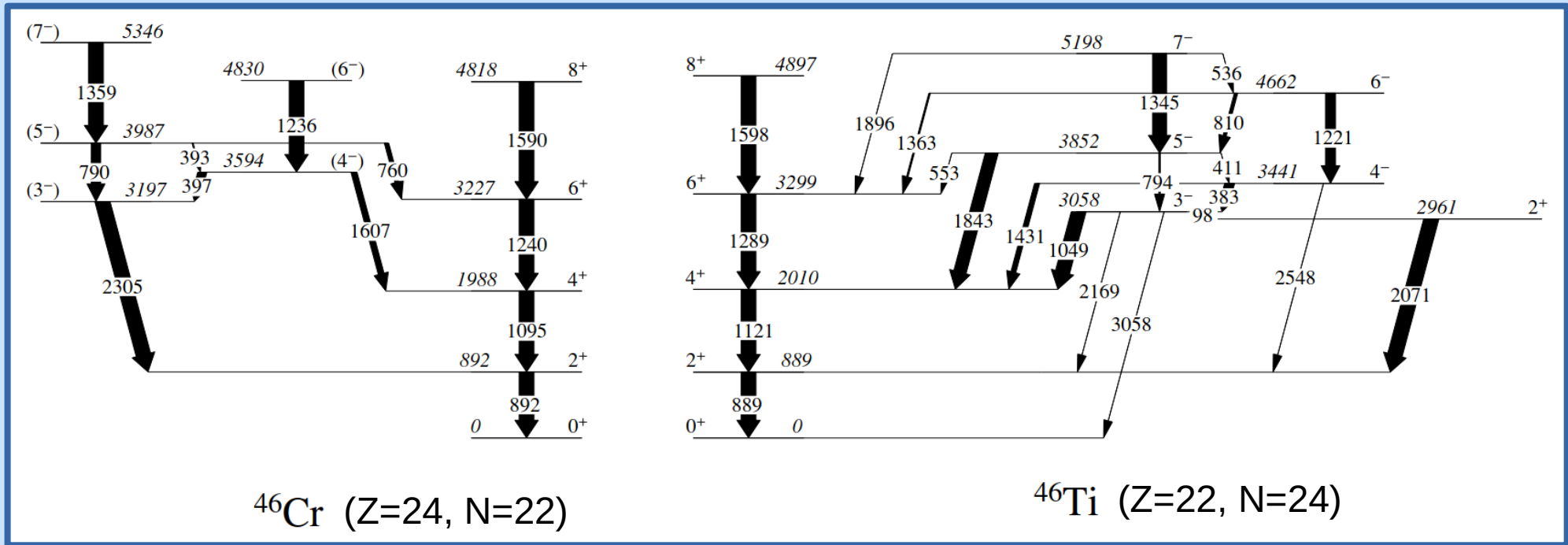
Correction for recoil energy



E_γ (keV)	% reduced using x and TOF
1120 (^{46}Ti)	69(2)
424 (^{46}V)	40.5(4)

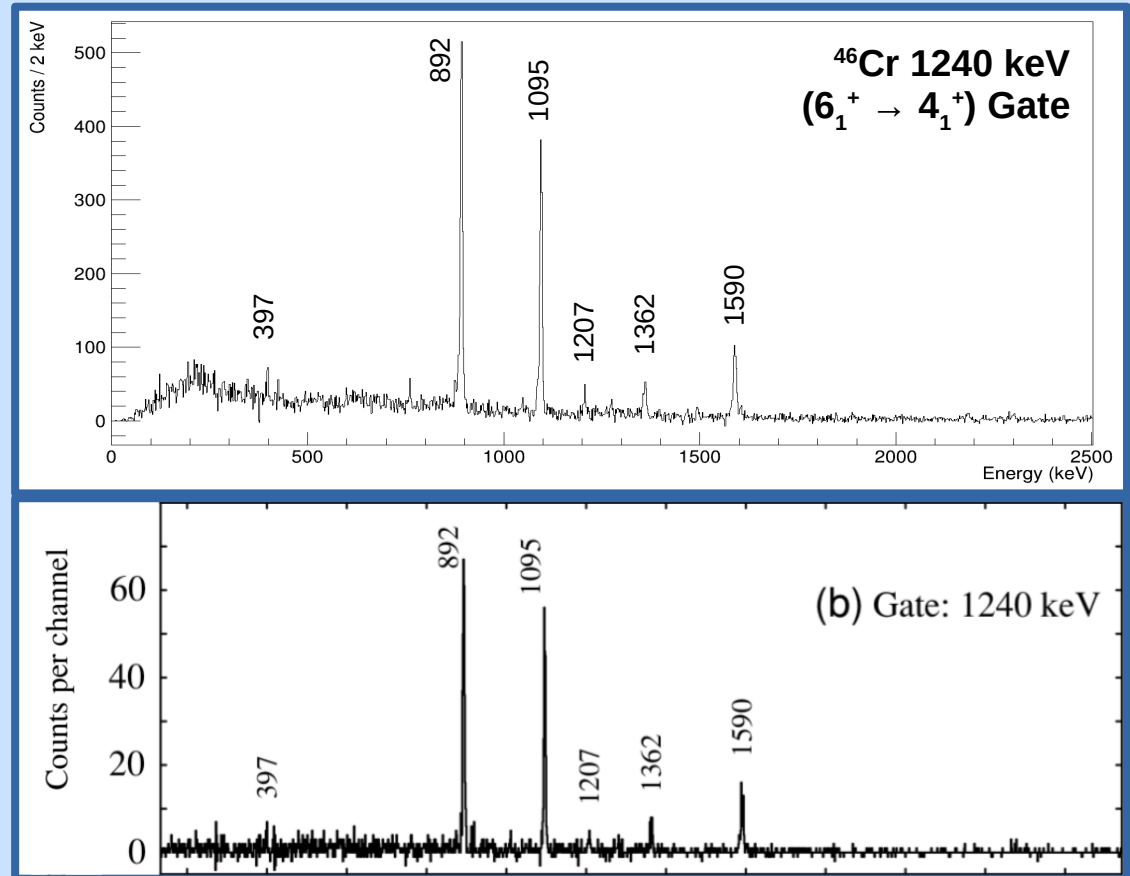
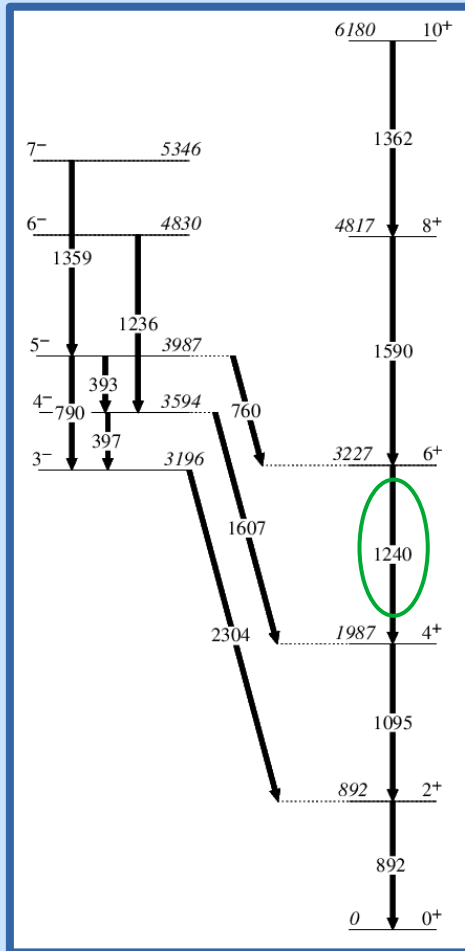
Mirror Nucleus Comparison

$T = 1, A = 46$ Mirror Pair



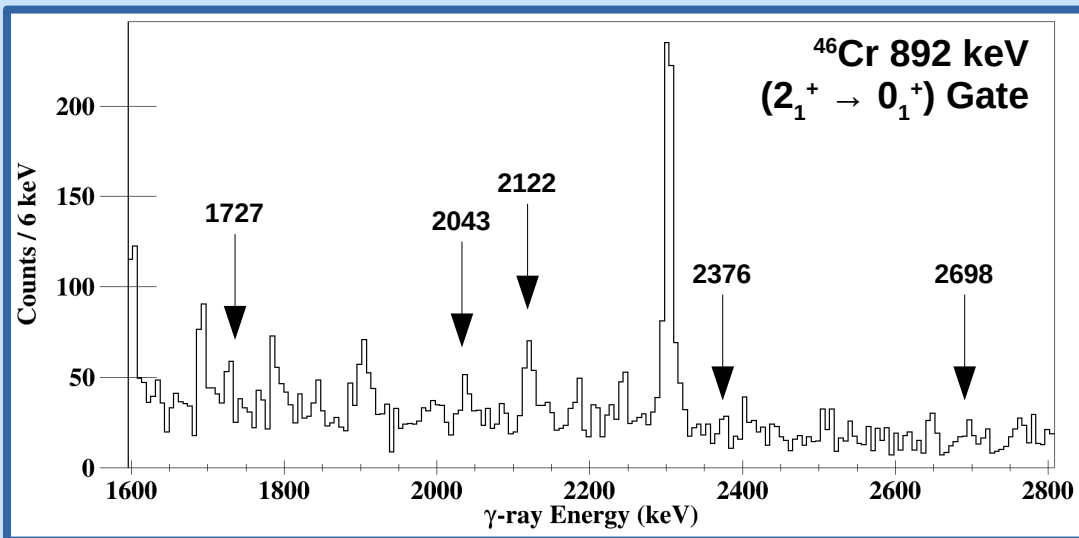
Garrett, P. E., et al. PRC 75.1 (2007): 014307.

Results – Previous Studies Comparison



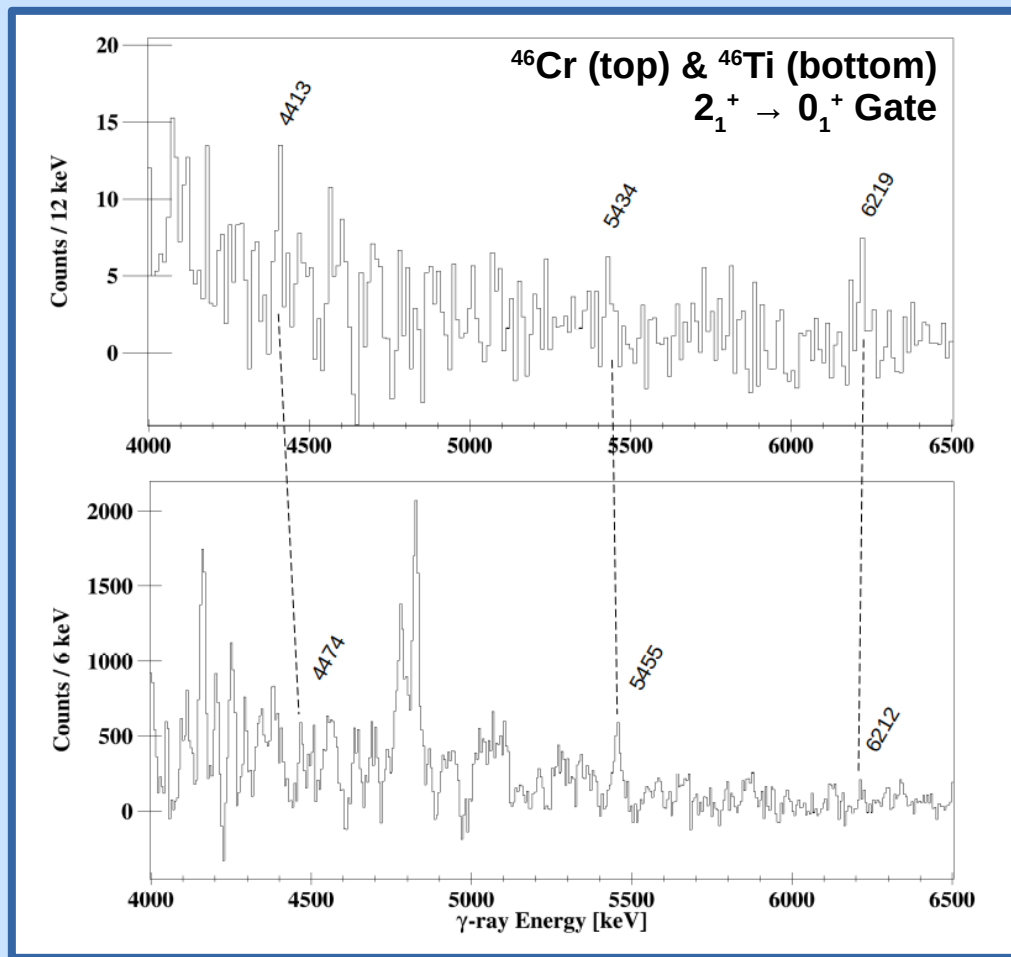
Garrett, P. E., et al. PRC 75.1 (2007): 014307.

Results – Resonance States



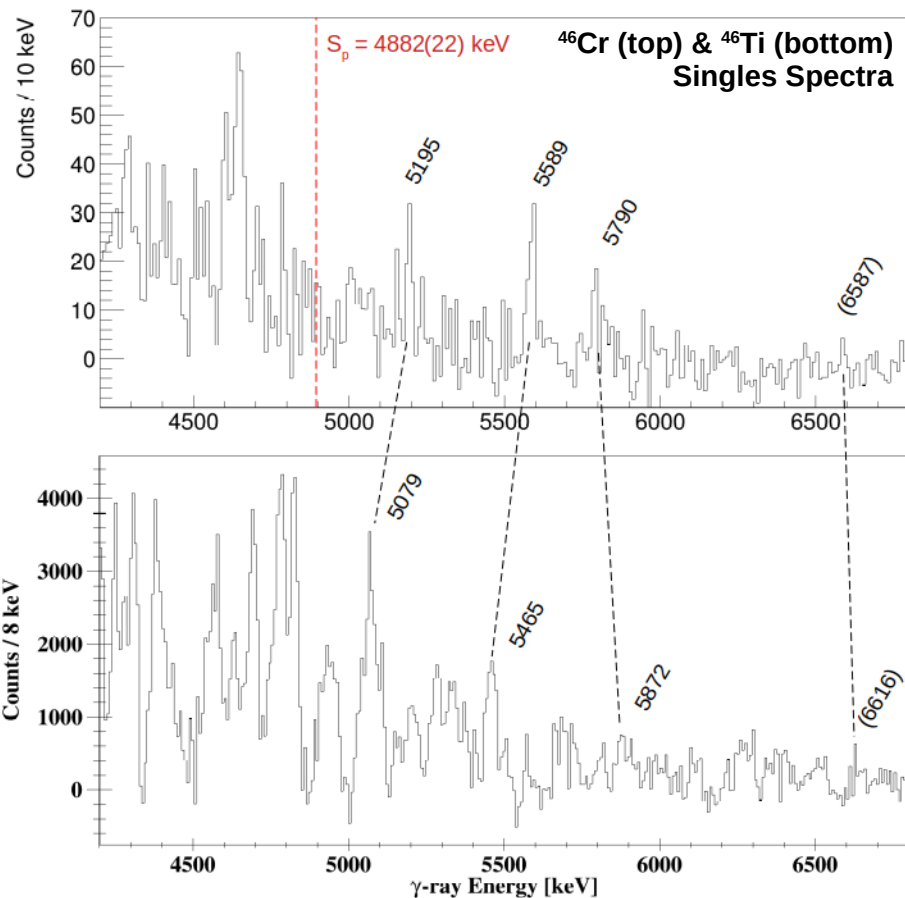
E_x (keV)	J^π	E_γ (keV)	Mirror E_x (keV)
892.24(5)	2^+	892.24(5)	889
1987.4(1)	4^+	1095.1(1)	2010
2619(1)	0^+	1727(1) *	2611
2935(2)	2^+	2043(3) *	2962
3014.1(5)	1^-	2121.8(5) *	3168
3196.0(3)	3^-	259(2)	3058
		2303.7(3)	
3227.0(2)	6^+	1239.6(2)	3299
3268(3)		2376(3) *	3212
3298.3(8)	2^+	2405(1)	3236
		3299(1)	
3494.4(5)	3^-	1507.0(5)	3569
3590(2)	0^+	2698(2) *	3572
3593.0(4)	4^-	397.2(4)	3441
		1605.5(6)	
5195(2)	2^+	5195(2)	5079
5305(5)	2^+	4413(5)	5363
5327(8)	3^-	2313(8)	5530
5588(2)	2^+	5587(2)	5465
5792(2)	2^+	5792(2)	5872
5826(8)	4^+	2812(8)	5994
6326(6)	4^+	5434(5)	6344
6587(3)	2^+	6587(3)	6629
6614(9)	3^-	3600(9)	6458
7111(6)	4^+	6219(6)	7104

Results – Resonance States



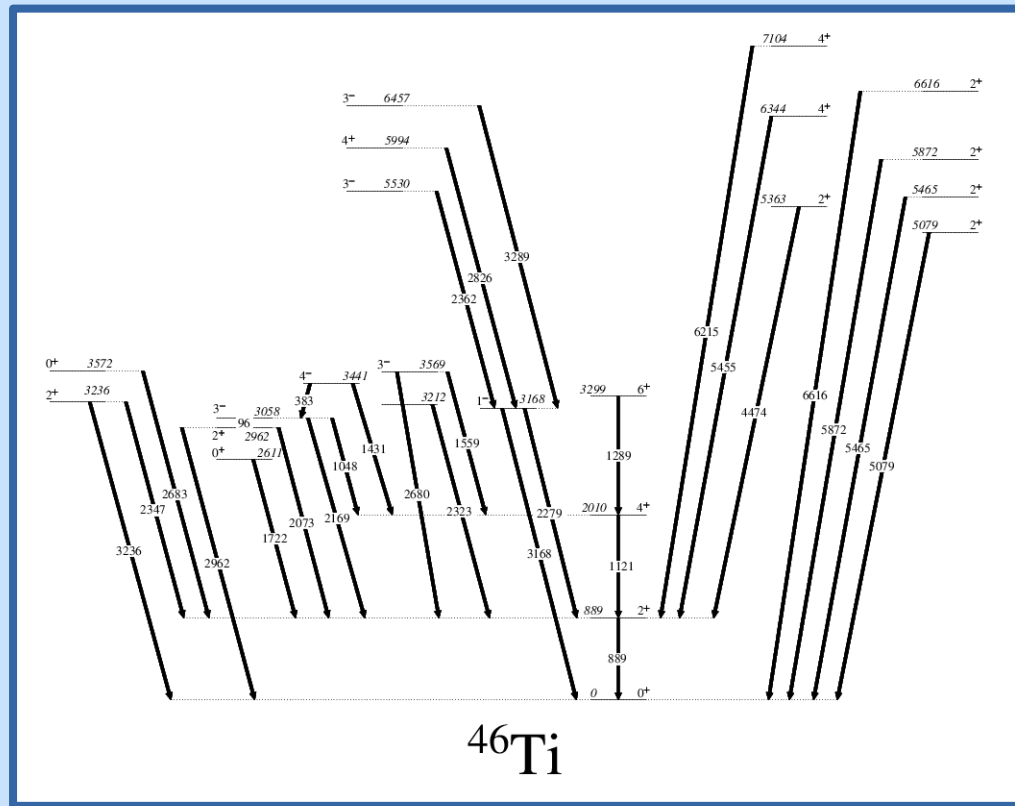
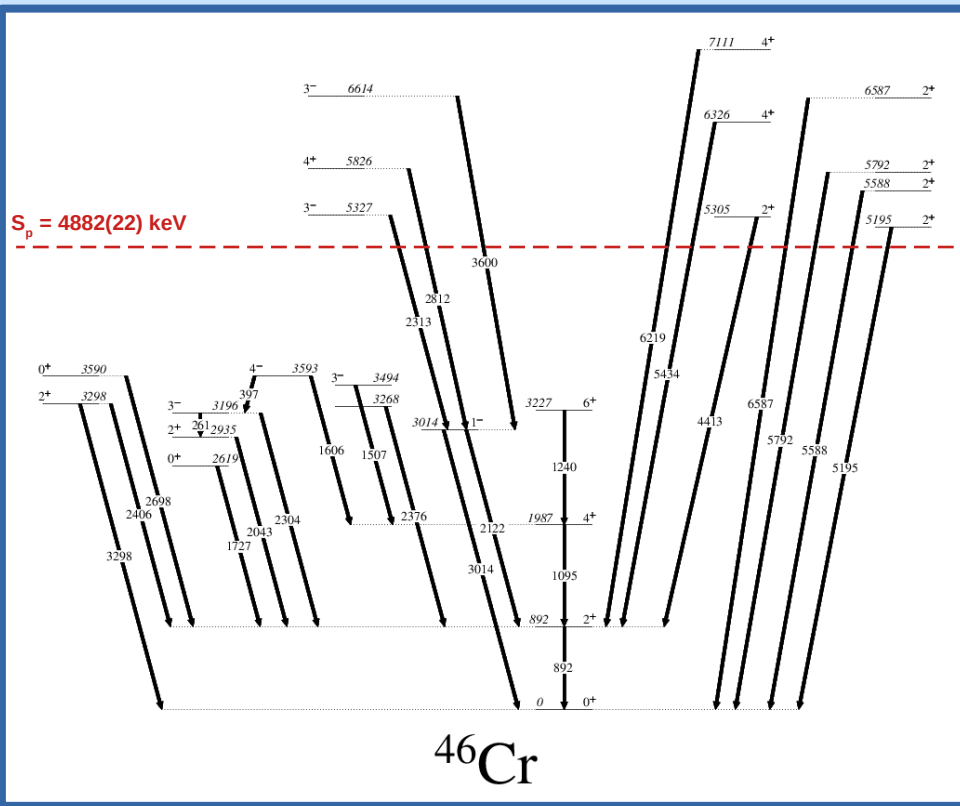
E_x (keV)	J^π	E_γ (keV)	Mirror E_x (keV)
892.24(5)	2^+	892.24(5)	889
1987.4(1)	4^+	1095.1(1)	2010
2619(1)	0^+	1727(1)	2611
2935(2)	2^+	2043(3)	2962
3014.1(5)	1^-	2121.8(5)	3168
3196.0(3)	3^-	259(2)	3058
		2303.7(3)	
3227.0(2)	6^+	1239.6(2)	3299
3268(3)		2376(3)	3212
3298.3(8)	2^+	2405(1)	3236
		3299(1)	
3494.4(5)	3^-	1507.0(5)	3569
3590(2)	0^+	2698(2)	3572
3593.0(4)	4^-	397.2(4)	3441
		1605.5(6)	
5195(2)	2^+	5195(2)	5079
5305(5)	2^+	4413(5) *	5363
5327(8)	3^-	2313(8)	5530
5588(2)	2^+	5587(2)	5465
5792(2)	2^+	5792(2)	5872
5826(8)	4^+	2812(8)	5994
6326(6)	4^+	5434(5) *	6344
6587(3)	2^+	6587(3)	6629
6614(9)	3^-	3600(9)	6458
7111(6)	4^+	6219(6) *	7104

Results – Resonance States

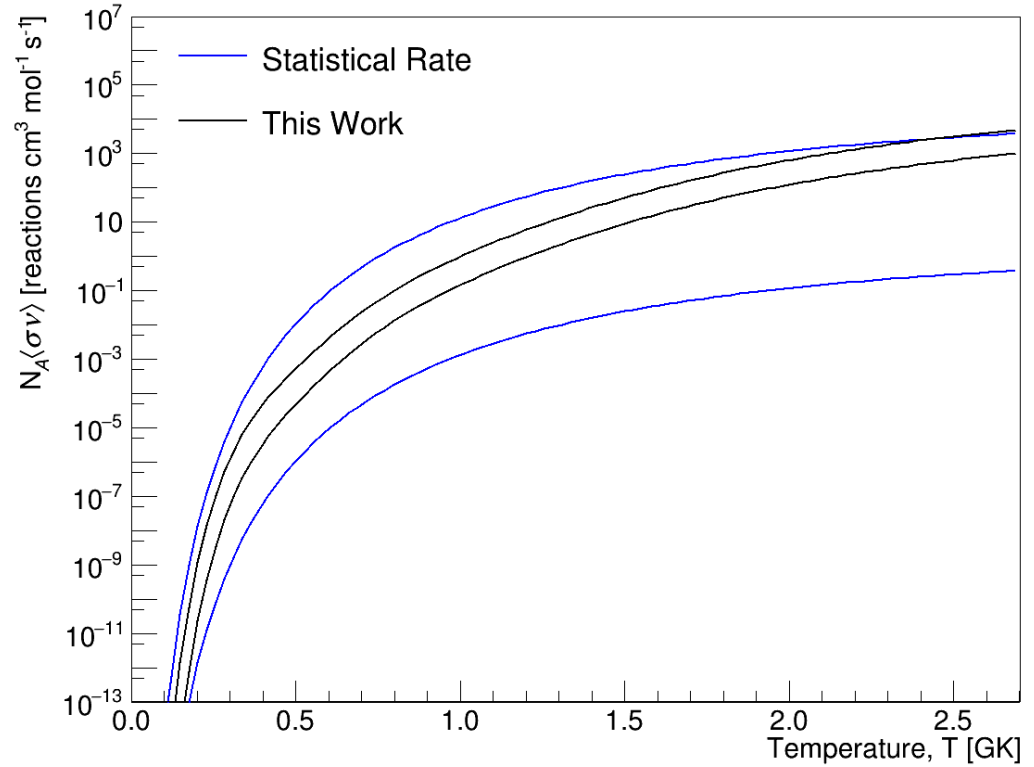
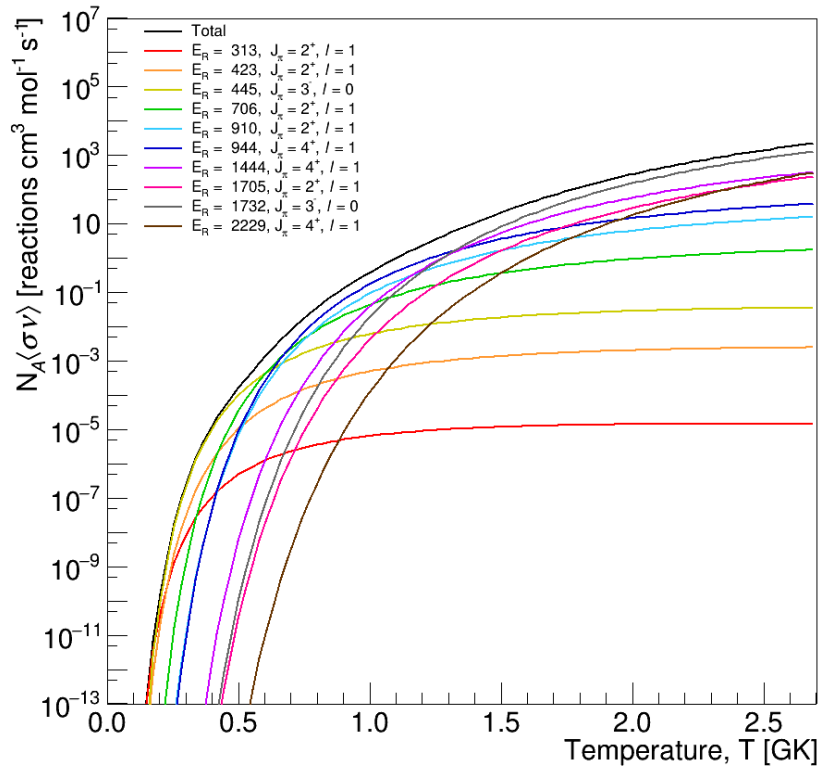


E_x (keV)	J^π	E_γ (keV)	Mirror E_x (keV)
892.24(5)	2^+	892.24(5)	889
1987.4(1)	4^+	1095.1(1)	2010
2619(1)	0^+	1727(1)	2611
2935(2)	2^+	2043(3)	2962
3014.1(5)	1^-	2121.8(5)	3168
3196.0(3)	3^-	259(2)	3058
		2303.7(3)	
3227.0(2)	6^+	1239.6(2)	3299
3268(3)		2376(3)	3212
3298.3(8)	2^+	2405(1)	3236
		3299(1)	
3494.4(5)	3^-	1507.0(5)	3569
3590(2)	0^+	2698(2)	3572
3593.0(4)	4^-	397.2(4)	3441
		1605.5(6)	
5195(2)	2^+	5195(2) *	5079
5305(5)	2^+	4413(5)	5363
5327(8)	3^-	2313(8)	5530
5588(2)	2^+	5587(2) *	5465
5792(2)	2^+	5792(2) *	5872
5826(8)	4^+	2812(8)	5994
6326(6)	4^+	5434(5)	6344
6587(3)	2^+	6587(3) *	6629
6614(9)	3^-	3600(9)	6458
7111(6)	4^+	6219(6)	7104

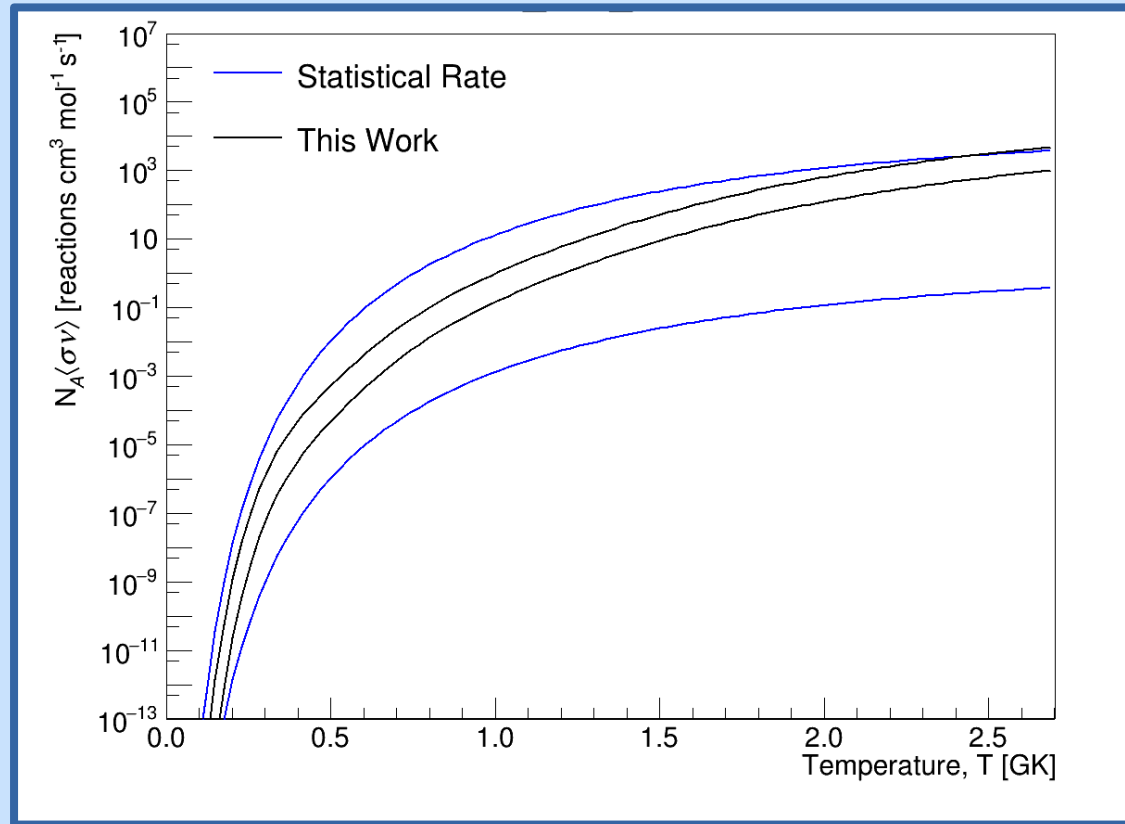
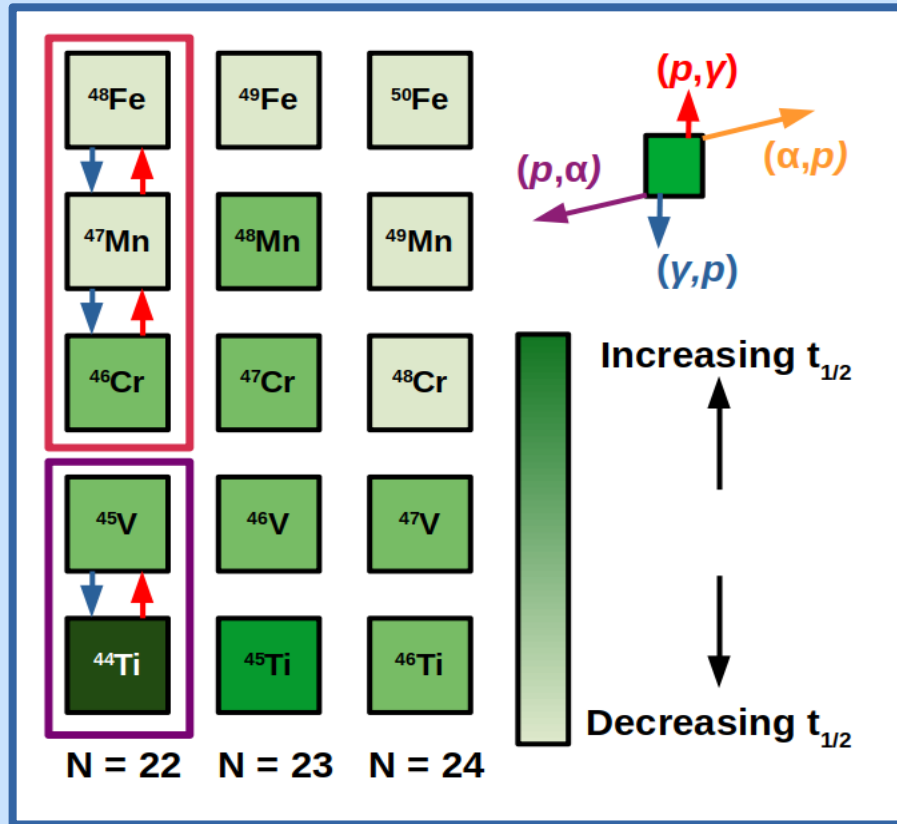
Results – Partial Level Scheme



Results – Reaction Rate



Results – Reaction Rate



Summary and Future Work

- $^{45}\text{V}(p,\gamma)^{46}\text{Cr}$ reaction rate is key to the destruction of ^{44}Ti during the α -rich freeze-out of CCSN
- First identification of 17 γ -rays, leading to observation of 10 proton-unbound states in ^{46}Cr
- Towards upper limit of previously known rate – more ^{44}Ti flows out of ^{44}Ti - ^{45}V cluster
- Finalise reaction rate; compare resonance states to shell model calculations
- Transfer reaction to get C^{2+}S , mass measurement of ^{46}Cr

Acknowledgments

G. Lotay¹, C. Campbell², L. Canete¹, M.P. Carpenter³, W.N. Catford¹, K.A. Chipps⁴, D.T. Doherty¹, J. Henderson¹, J. José⁵, A.R.L. Kennington¹, T. Lauritsen³, J. Li², M. Moukaddam⁶, C. Müller-Gatermann³, C. O'Shea¹, S.D. Pain⁴, C. Paxman¹, B.J. Reed¹, P.H. Regan¹, W. Reviol³, D.Seweryniak³, M. Siciliano³, G.L. Wilson^{3,7}, S. Zhu⁸

¹Department of Physics, University of Surrey, Guildford, Surrey, GU2 7XH. UK

²Lawrence Berkeley National Laboratory, Berkeley, CA 94720, USA

³Argonne National Laboratory, Argonne, Illinois 60439, USA

⁴Oak Ridge National Laboratory, Oak Ridge, Tennessee 37831, USA

⁵Universitat Politècnica De Catalunya, 08034 Barcelona, Spain

⁶Université de Strasbourg, IPHC, 67037 Strasbourg, France

⁷Louisiana State University, Baton Rouge, Louisiana 70803, USA

⁸Brookhaven National Laboratory, National Nuclear Data Center, New York 11973, USA

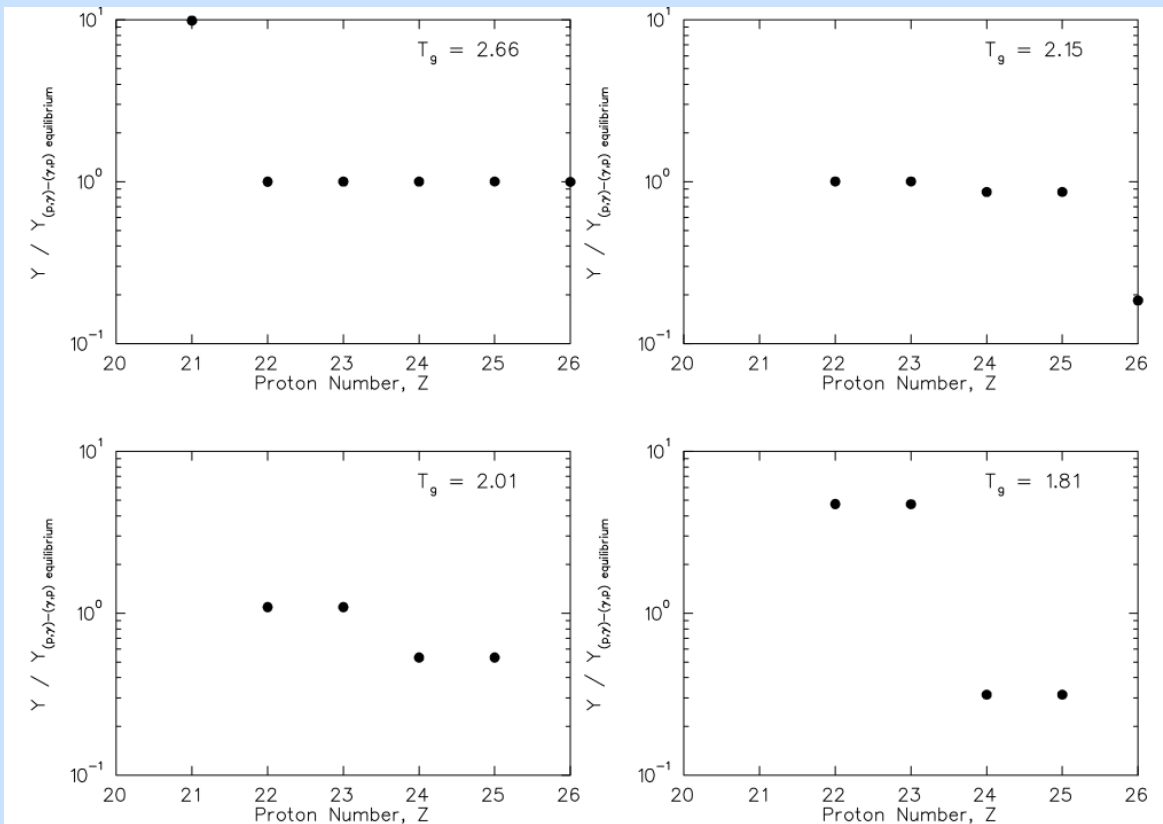


FIG. 13.—Evolution of the (p, γ) – (γ, p) equilibrium for the $N = 22$ isotones as the temperature falls, with the standard $^{45}\text{V}(p, \gamma)^{46}\text{Cr}$ rate. The ^{44}Ti and ^{45}V pair ($Z = 22$ and 23) increasingly depart from equilibrium with the ^{46}Cr and ^{47}Mn ($Z = 24$ and 25) as the temperature declines.

TABLE 5

ORDER OF IMPORTANCE OF
REACTIONS PRODUCING
 ^{44}Ti AT $\eta = 0^a$

Reaction	Slope
$^{44}\text{Ti}(\alpha, p)^{47}\text{V}$	−0.394
$\alpha(2\alpha, \gamma)^{12}\text{C}$	+0.386
$^{45}\text{V}(p, \gamma)^{46}\text{Cr}$	−0.361
$^{40}\text{Ca}(\alpha, \gamma)^{44}\text{Ti}$	+0.137
$^{57}\text{Co}(p, n)^{57}\text{Ni}$	+0.102
$^{36}\text{Ar}(\alpha, p)^{39}\text{K}$	+0.037
$^{44}\text{Ti}(\alpha, \gamma)^{48}\text{Cr}$	−0.024
$^{12}\text{C}(\alpha, \gamma)^{16}\text{O}$	−0.017
$^{57}\text{Ni}(p, \gamma)^{58}\text{Cu}$	+0.013
$^{58}\text{Cu}(p, \gamma)^{59}\text{Zn}$	+0.011
$^{36}\text{Ar}(\alpha, \gamma)^{40}\text{Ca}$	+0.008
$^{44}\text{Ti}(p, \gamma)^{45}\text{V}$	−0.005
$^{57}\text{Co}(p, \gamma)^{58}\text{Ni}$	+0.002
$^{57}\text{Ni}(n, \gamma)^{58}\text{Cu}$	+0.002
$^{54}\text{Fe}(\alpha, n)^{57}\text{Ni}$	+0.002
$^{40}\text{Ca}(\alpha, p)^{43}\text{Sc}$	−0.002

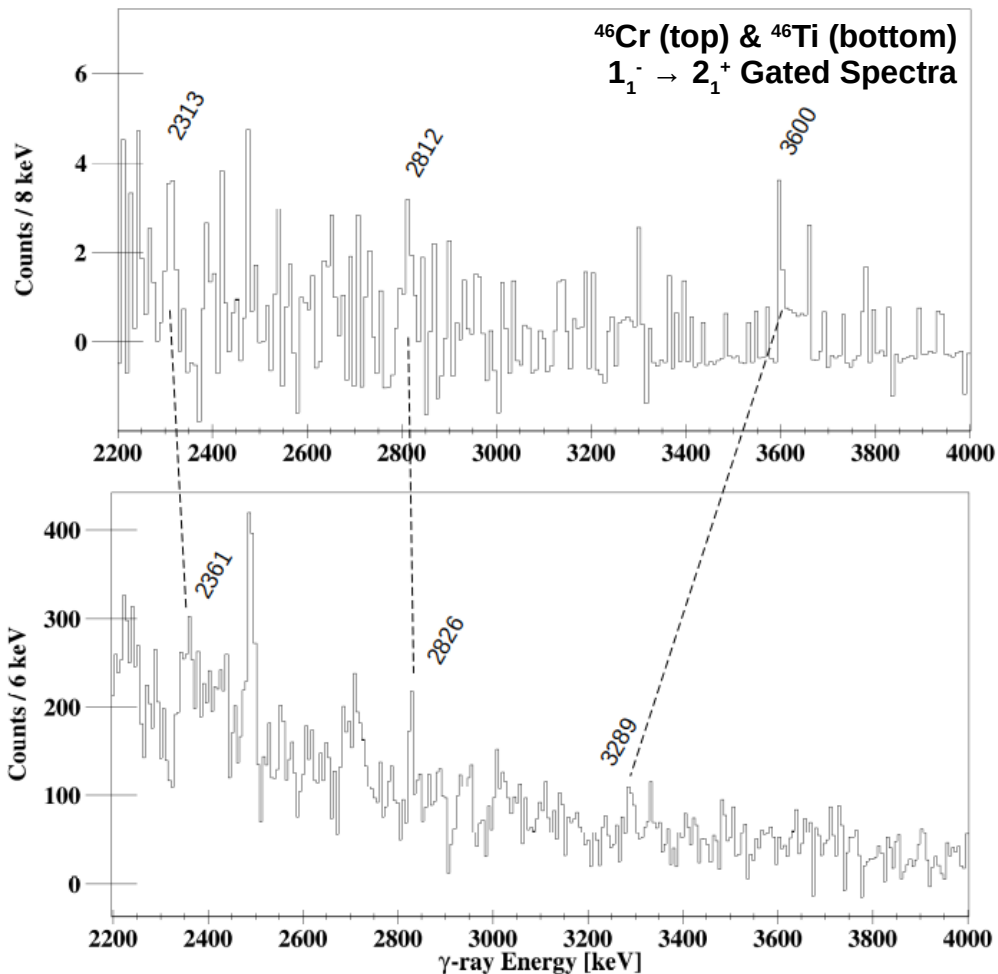
^a Order of importance of reactions producing ^{44}Ti at $\eta = 0$ according to the slope of $X(^{44}\text{Ti})$ near the standard reaction rates.

Clayton, D.D., Jin, L. and Meyer, B.S., 1998. Nuclear reactions governing the nucleosynthesis of ^{44}Ti . The Astrophysical Journal, 504(1), p.500.

TABLE 4
ORDER OF IMPORTANCE OF REACTIONS PRODUCING ^{44}Ti AT $\eta = 0$

REACTION RATE MULTIPLIED BY 1/100			REACTION RATE MULTIPLIED BY 100	
RANK	Reaction	^{44}Ti Change (percent)	Reaction	^{44}Ti Change (percent)
1	$^{44}\text{Ti}(\alpha, p)^{47}\text{V}$	+173	$^{45}\text{V}(p, \gamma)^{46}\text{Cr}$	-98
2	$\alpha(2\alpha, \gamma)^{12}\text{C}$	-100	$\alpha(2\alpha, \gamma)^{12}\text{C}$	+67
3	$^{40}\text{Ca}(\alpha, \gamma)^{44}\text{Ti}$	-72	$^{44}\text{Ti}(\alpha, p)^{47}\text{V}$	-89
4	$^{45}\text{V}(p, \gamma)^{46}\text{Cr}$	+57	$^{44}\text{Ti}(\alpha, \gamma)^{48}\text{Cr}$	-61
5	$^{57}\text{Ni}(p, \gamma)^{58}\text{Cu}$	-47	$^{57}\text{Co}(p, n)^{57}\text{Ni}$	+25
6	$^{57}\text{Co}(p, n)^{57}\text{Ni}$	-33	$^{40}\text{Ca}(\alpha, \gamma)^{44}\text{Ti}$	+22
7	$^{13}\text{N}(p, \gamma)^{14}\text{O}$	-16	$^{57}\text{Ni}(n, \gamma)^{58}\text{Ni}$	+10
8	$^{58}\text{Cu}(p, \gamma)^{59}\text{Zn}$	-14	$^{54}\text{Fe}(\alpha, n)^{57}\text{Ni}$	+9.4
9	$^{36}\text{Ar}(\alpha, p)^{39}\text{K}$	-11	$^{36}\text{Ar}(\alpha, p)^{39}\text{K}$	+5.5
10	$^{12}\text{C}(\alpha, \gamma)^{16}\text{O}$	+3.5	$^{36}\text{Ar}(\alpha, \gamma)^{40}\text{Ca}$	+5.3

Clayton, D.D., Jin, L. and Meyer, B.S., 1998. Nuclear reactions governing the nucleosynthesis of ^{44}Ti . The Astrophysical Journal, 504(1), p.500.



E_x (keV)	J^π	E_γ (keV)	Mirror E_x (keV)
892.24(5)	2^+	892.24(5)	889
1987.4(1)	4^+	1095.1(1)	2010
2619(1)	0^+	1727(1)	2611
2935(2)	2^+	2043(3)	2962
3014.1(5)	1^-	2121.8(5)	3168
3196.0(3)	3^-	259(2)	3058
		2303.7(3)	
3227.0(2)	6^+	1239.6(2)	3299
3268(3)		2376(3)	3212
3298.3(8)	2^+	2405(1)	3236
		3299(1)	
3494.4(5)	3^-	1507.0(5)	3569
3590(2)	0^+	2698(2)	3572
3593.0(4)	4^-	397.2(4)	3441
		1605.5(6)	
5195(2)	2^+	5195(2)	5079
5305(5)	2^+	4413(5)	5363
5327(8)	3^-	2313(8) *	5530
5588(2)	2^+	5587(2)	5465
5792(2)	2^+	5792(2)	5872
5826(8)	4^+	2812(8) *	5994
6326(6)	4^+	5434(5)	6344
6587(3)	2^+	6587(3)	6629
6614(9)	3^-	3600(9) *	6458
7111(6)	4^+	6219(6)	7104

PACE4 Calculations

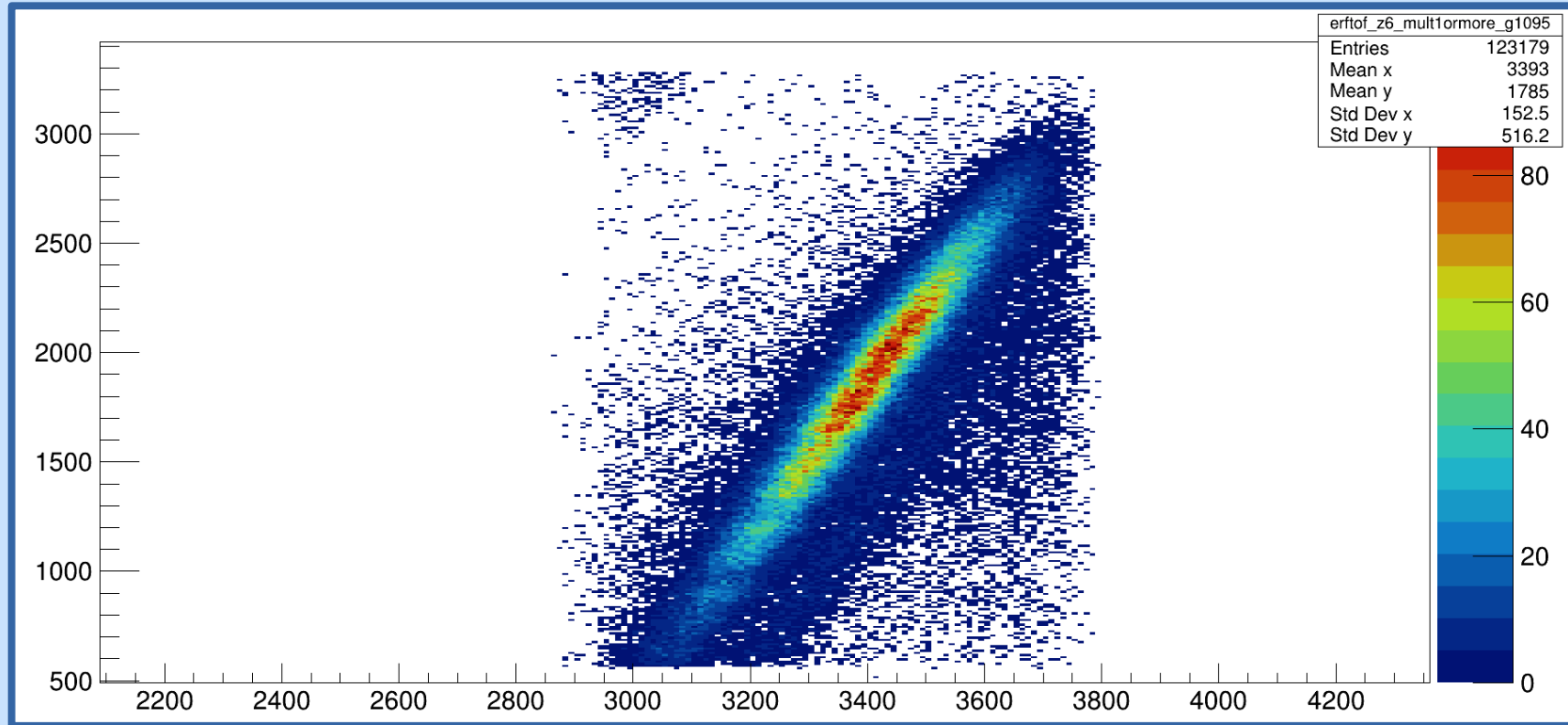
On ^{12}C

1. Yields of residual nuclei					
Z	N	A	events	percent	x-section(mb)
24	23	47 Cr	63	0.063%	0.595
23	24	47 V	380	0.38%	3.59
24	22	46 Cr	25	0.025%	0.236
23	23	46 V	18520	18.5%	175
22	24	46 Ti	28646	28.6%	270
23	22	45 V	10	0.01%	0.0944
22	23	45 Ti	16937	16.9%	160
21	24	45 Sc	5540	5.54%	52.3
22	22	44 Ti	1193	1.19%	11.3
22	21	43 Ti	364	0.364%	3.44
21	22	43 Sc	16405	16.4%	155
21	21	42 Sc	44	0.044%	0.415
20	22	42 Ca	397	0.397%	3.75
20	20	40 Ca	9020	9.02%	85.2
19	20	39 K	2455	2.46%	23.2
TOTAL			99999	100	944.208

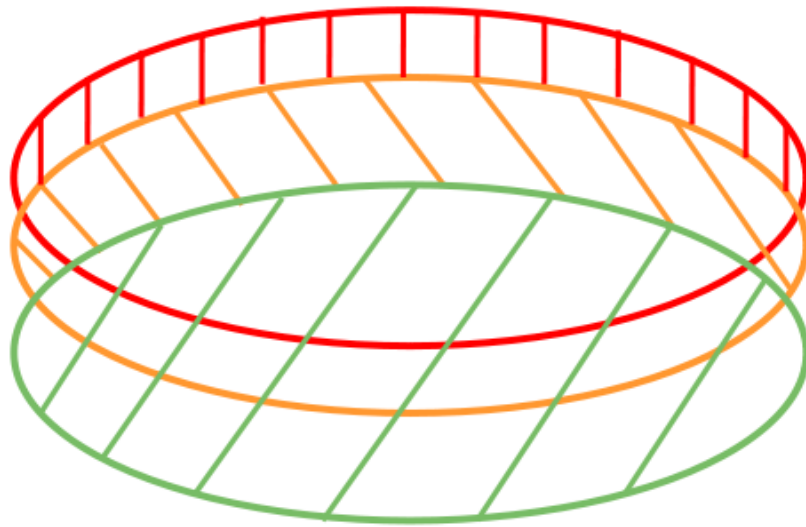
On ^{16}O

1. Yields of residual nuclei					
Z	N	A	events	percent	x-section(mb)
26	25	51 Fe	3	0.003%	0.0276
25	26	51 Mn	21	0.021%	0.193
26	24	50 Fe	33	0.033%	0.303
25	25	50 Mn	3489	3.49%	32.1
24	26	50 Cr	5878	5.88%	54.1
25	24	49 Mn	247	0.247%	2.27
24	25	49 Cr	40569	40.6%	373
23	26	49 V	15421	15.4%	142
24	24	48 Cr	235	0.235%	2.16
23	25	48 V	600	0.6%	5.52
22	26	48 Ti	8	0.008%	0.0736
24	23	47 Cr	686	0.686%	6.31
23	24	47 V	14657	14.7%	135
23	23	46 V	2222	2.22%	20.4
22	24	46 Ti	12585	12.6%	116
22	23	45 Ti	11	0.011%	0.101
21	24	45 Sc	3	0.003%	0.0276
22	22	44 Ti	2326	2.33%	21.4
21	22	43 Sc	932	0.932%	8.57
20	20	40 Ca	73	0.073%	0.671
TOTAL			99999	100	919.564


TOF Dependence on Recoil Energy




X-RFTOF Gates





 - 46Cr xrftof cut

 - 46V xrftof cut

 - 46Ti xrftof cut

 1) in 46Cr cut

 2) in 46V cut and not in 46Cr cut

 3) in 46Ti cut and not in 46V and 46Cr cuts

Decay Channels

- Why neutron-deficient compound nuclei emit neutron over protons in fusion-evaporation

Near stable (compound) nuclei, $S_p \sim S_n \sim 5-8$ MeV.
Coulomb barrier means (HI,xn) favoured over (HI,xp)

Very neutron-deficient (compound) nuclei,
e.g. ^{136}Gd , $S_p = 2.15$ MeV, $S_n = 12.94$ MeV

